Inorganic Chemistry

pubs.acs.org/IC Article

Role of the Trifluoropropynyl Ligand in Blue-Shifting Charge-Transfer States in Emissive Pt Diimine Complexes and an Investigation into the PMMA-Imposed Rigidoluminescence and Rigidochromism

Jackson S. McCarthy, Mary Jo McCormick, John H. Zimmerman, H. Rhodes Hambrick, Wilson M. Thomas, Colin D. McMillen, and Paul S. Wagenknecht*



Cite This: Inorg. Chem. 2022, 61, 11366–11376



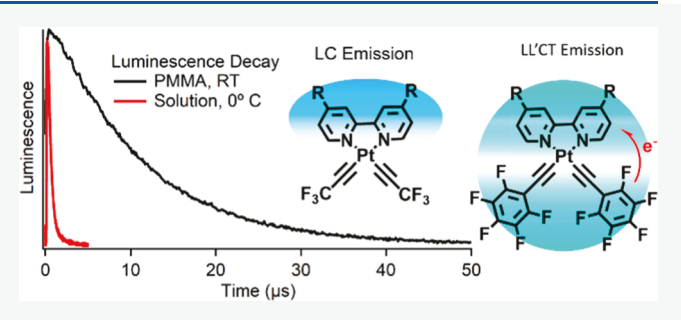
ACCESS

III Metrics & More

Article Recommendations

Supporting Information

ABSTRACT: Square-planar Pt^{II} complexes are of interest as dopants for the emissive layer of organic light-emitting diodes. Herein, the photophysics of three Pt bipyridyl complexes with the strongly e⁻ withdrawing, high-field, 3,3,3-trifluoropropynyl ligand has been investigated. One complex, (phbpy)PtC₂CF₃ (phbpy = 6-phenyl-2,2'-dipyridyl), has also been characterized by single-crystal X-ray diffraction. All complexes reported are emissive in both RT CH₂Cl₂ solution (Φ_{PL} = 0.007 to 0.027) and PMMA film (Φ_{PL} = 0.25 to 0.42). The trifluoropropynyl ligand elevates the energy of the MLCT and LL'CT states above that of the IL π - π * state, resulting in IL emission in all cases. The emission energies of the



trifluoropropynyl compounds are also blue-shifted relative to the analogous pentafluorophenylethynyl compounds, suggesting that the trifluoropropynyl ligand is one of the most electron-withdrawing alkynyl ligands. Rate constants for radiative and nonradiative deactivation were determined from experimentally determined values of Φ_{PL} and excited-state lifetimes in both solution and PMMA films. The increase in Φ_{PL} upon incorporation into PMMA film (rigidoluminescence) results from a decrease in the rate constant for non-radiative relaxation. Experimental activation energies for excited-state decay in combination with TDDFT are consistent with the rigidoluminescence resulting from an increase in the energy of the non-emissive triplet metal-centered state. Two of the complexes investigated, (Ph2 bpy)Pt(C_2CF_3)₂ and ($^{t-Bu2}$ bpy)Pt(C_2CF_3)₂, where $^{t-Bu2}$ bpy = 4,4'-di-tert-butyl-2,2'-dipyridyl and Ph2 bpy = 4,4'-diphenyl-2,2'-dipyridyl, exhibit concentration-dependent excimer emission (orange) along with monomer emission (blue), enabling fine-tuning of the emission color. However, excimer emission was absent in cured PMMA films up to the solubility limit for solution processing of (Ph2 bpy)Pt(C_2CF_3)₂ in CH₂Cl₂, demonstrating the diffusional nature of excimer formation.

INTRODUCTION

Recent investigations into emissive materials for organic lightemitting diodes (OLEDs) suggest that phosphorescent emitters improve device efficiency due to their ability to harvest both singlet and triplet excitons. 1-5 Complexes of Ir III and Pt^{II} have been of particular interest due to strong spinorbit coupling (SOC) induced by third-row transition metals.^{4–9} Although a range of highly efficient OLEDs using phosphorescent organometallic species that emit in the greento-red portion of the spectrum have been reported, 10-12 efficient deep-blue emission with good color purity is still considered technologically challenging. Lowered efficiency is due, in part, to the presence of triplet metal-centered (³MC) states that become increasingly thermally accessible from the emissive state as the emission energy is blue-shifted. Such ³MC states are known to undergo rapid, nonradiative deactivation. Therefore, their accessibility serves as a nonradiative sink (Figure 1a). 13-17 Destabilizing the 3MC states through the use

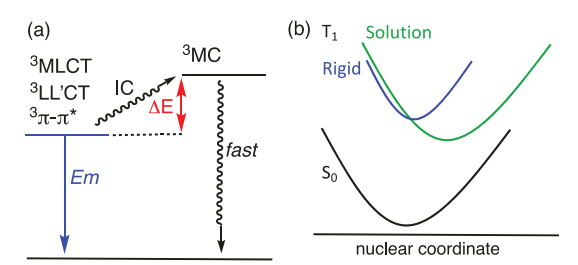


Figure 1. (a) Modified Jablonski diagram for typical organometallic chromophores with accessible 3MC states. (b) Potential well diagram for a complex with an excited-state nuclear distortion in solution vs the same complex in a rigid environment.

Received: May 6, 2022 Revised: June 29, 2022 Accepted: June 30, 2022 Published: July 12, 2022



of high-field ligands is typically utilized to overcome this limitation, and several $\rm Ir^{III}$ and $\rm Pt^{II}$ complexes with efficient deep-blue emission have been prepared. $^{16,18-22}$

Emissive Pt^{II} complexes are typically square-planar complexes involving combinations of substituted bipyridyl ligands, $^{22-31}$ cyclometallating (C^N) or (C^N^N) ligands, $^{32-35}$ alkynyl ligands, $^{23,27,28,31,35-38}$ and N-heterocyclic carbene (NHC) ligands. The high-field anionic carbanion ligands raise the energy of the ^{3}MC states well above that of the emissive state, thus increasing photoluminescence quantum yields $(\Phi_{PL})^{21,39}$ Emission in such systems may occur from a metal-to-ligand charge-transfer ($^{3}MLCT$) state, 23,32,40 a ligand-to-ligand charge-transfer ($^{3}LL'CT$) state, 33 a ligand-centered (^{3}LC) state such as $^{3}\pi-\pi^{*}$ state, 18,27,40 or a state of mixed origin, 33 depending on which of these states is lowest in energy (Figure 1a).

For use in OLED devices, such emissive complexes are suspended in thin polymer films and the rigidification often results in noteworthy modification of the photophysical properties. Chiefly, $\Phi_{\rm pl}$ and emission lifetimes (τ) in polymethylmethacrylate (PMMA) films can increase by up to two orders of magnitude, 18,33,41 which is a form of rigidoluminescence. There is sometimes an associated blue shift of the emission, ^{24,32} which is a form of rigidochromism. For example, a recent study demonstrated that incorporation of an Ir phosphor into PMMA film increases Φ_{PL} up to 23-fold and induces blue shifts in emission, exceeding 450 cm⁻¹.41 These impacts can be so significant that the characterization of phosphors for possible OLED use should typically be augmented with thin film investigations as behavior in film is more representative of possible device performance. 13,41 Though the rigidoluminescence can suggest either an increase in the radiative rate constant, k_r , or a decrease in the nonradiative rate constant, k_{nr} , the latter typically dominates. Thus, explanations for increased Φ_{PL} and lifetimes in PMMA film have typically focused on the nonradiative mechanism, 13,14,16,18,41,42 though in some situations, a dominant increase in k_r has been linked to immobilization-induced increases in excited-state (ES) SOC.41

Rigidochromism and rigidoluminescence are often closely related, inasmuch as both are related to the increase in the ES energy that occurs when a complex is prevented from relaxing to its equilibrium geometry (Figure 1b). Chiefly, upon vertical excitation in solution, immediate vibrational relaxation results in a new equilibrium geometry (Figure 1b, green). The extent of this distortion depends on the ES electron distribution. For example, ³MC states typically populate M-L antibonding orbitals and result in significant M-L bond elongation, whereas ${}^{3}\pi-\pi^{*}$ states undergo very little distortion. Likewise, MLCT states are typically more distorted than $\pi - \pi^*$ states.⁴³ The stabilization that accompanies the distortion is prevented in rigid media (Figure 1b, blue), resulting in a higher-energy ES. 44-47 Consequently, the emission will be blue-shifted in rigid media, and the extent of the shift is dependent on the magnitude of solution-phase distortion. 24,28,44–46 Thus, relative magnitudes of the rigidochromic shift can be an indicator of relative ES distortions, thereby assisting in assigning ES orbital character. Rigidoluminescence for a range of complexes where thermal access of the ³MC state dominates the nonradiative decay pathway is related to rigidochromic shifts as follows: the increase in the energy of the ³MC state that accompanies rigidification will lead to an increase in ΔE (Figure 1a), thus decreasing access to the nonradiative ³MC state. In turn, this

may decrease $k_{\rm nr}$, increasing $\Phi_{\rm PL}$ and τ in rigid media, such as PMMA film. Perhaps, the earliest recognition that $^3{\rm MC}$ states could be rendered inaccessible in rigid medium involved immobilization of ${\rm Ru(bpy)_3}^{2+}$ in a cellulose acetate matrix. More recently, these rigidity effects have played an important role in the characterization of a range of emissive ${\rm Pt^{II}}$ complexes. 13,18,25,43,49

Clearly, both the ligand identity and the rigidity of the environment impact emission characteristics of phosphors for possible use in OLEDs. One ligand commonly used in blueshifting emission from MLCT or LL'CT ESs in alkynyl complexes is the pentafluorophenylethynyl ligand, $-C \equiv CC_6F_5$. Phis ligand lowers the HOMO due to the strong electron-withdrawing ability of the C₆F₅ substituent, leading to a larger HOMO-LUMO gap. Our group has recently shown that the trifluoropropynyl ligand, −C≡CCF₃, is both more electron-withdrawing and is a higher-field ligand than $-C \equiv CC_6F_5$. ⁵⁴ Thus, there is the possibility of raising the level of both the emissive state and the ³MC state, causing a blue shift in emission, while preserving Φ_{PL} . Herein, we present the synthesis and characterization of a series of square-planar Pt^{II} trifluoropropynyl complexes and compare them to those of the corresponding pentafluorophenylethynyl complexes^{23,32} (Figure 2). The emission spectra and computational

Figure 2. Complexes investigated herein, along with abbreviations used. Ligand abbreviations: ${}^{t\text{-Bu2}}\text{bpy} = 4,4'\text{-di-}\textit{tert-}\text{butyl-2,2'-dipyridyl};}$ Ph2bpy = 4,4'-diphenyl-2,2'-dipyridyl; phbpy = 6-phenyl-2,2'-dipyridyl.

investigations reveal the orbital character of the emissive state for all −C≡CCF₃ complexes investigated herein as being dominated by ³IL (bpy or phbpy) character. This characterization is consistent with the -C≡CCF₃ ligand raising the energy of the ³MLCT and ³LL'CT states above that of the ³IL state due to the strong electron-withdrawing nature of the CF₃ substituent. Thus, the -C≡CCF₃ ligand may be a useful ancillary ligand when IL emission is desired. For each complex, there is a significant increase in the emission quantum yield in PMMA film. Solution activation energies and computational investigations provide strong experimental evidence that rigidification raises the energy of the ³MC state, rendering that state less thermodynamically accessible. Lastly, at high concentrations, both monomer emission (blue) and excimer emission (orange) are present, resulting in warm-white emission. However, at these same concentrations in PMMA films, excimer emission is absent, clearly indicating the role of diffusion in the excimer emission.

■ EXPERIMENTAL SECTION

Materials and Methods. 3,3,3-Trifluoropropyne was obtained from Synquest Laboratories. Dichloromethane was dried and degassed with an Innovative Technologies solvent purification system before use. The Pt precursors, (f-Bu2bpy)PtCl₂, (Ph2bpy)PtCl₂, and

(phbpy)PtCl^{32,55} were prepared according to literature procedures. All reactions were carried out under air-free conditions using standard Schlenk techniques. NMR spectra were obtained using a Varian 400-MR or INOVA-500 spectrometer. Infrared spectra were obtained using a PerkinElmer Spectrum Two FT-IR spectrometer with a UATR attachment. Absorption spectra were collected using a Cary-50 UV-vis spectrophotometer. Emission spectra were collected using a Horiba Scientific Fluorolog-3 spectrofluorometer equipped with a FL-1013 liquid nitrogen dewar assembly for 77 K measurements and a J-1933 solid-sample holder for film measurements. Emission lifetimes were measured using a Photon Technology International (PTI) GL-3300 pulsed nitrogen laser fed into a PTI GL-302 dye laser as the excitation source. The resulting data set was collected on an OLIS SM-45 EM fluorescence lifetime measurement system using a Hamamatsu R928 photomultiplier tube fed through a variable feedthrough terminator into a LeCroy WaveJet 352A oscilloscope and analyzed using OLIS Spectral Works (lower lifetime limit = 200 ns). Temperature control was achieved using a TLC 50 cuvette holder (temperature range -28.5 to +105 °C) from Quantum Northwest. Relative solution-state Φ_{PL} were determined from ratios of the slope of the integrated emission intensity versus absorbance of the analyte versus a quinine sulfate standard. Film Φ_{PL} were measured using a Horiba K-Sphere Petite. PMMA films for spectroscopy were prepared either by doctor blading or by spin coating a solution of PMMA (123 mg, $M_{\rm W} \sim 120,000$) and the complex of study in CH₂Cl₂ (1 mL). PMMA films, unless otherwise stated, were made at the solubility limits of this method, which are 0.16, 1.8, and 1.0 wt % for 1CF₃, 2CF₃, and 3CF₃, respectively. Elemental analyses were performed by Midwest Microlabs.

Computational Methods. Gaussian 16^{56} was used for all DFT and time-dependent density functional theory (TDDFT) calculations. Computational models involved the functional B3LYP⁵⁷ and the basis sets $6\text{-}31G(d)^{58}$ and LANL2DZ.⁵⁹ GaussView version $6,^{60}$ was used for all orbital imaging. GaussSum 3^{61} was used for Mulliken population analysis.

X-ray Diffraction. Single crystals of (phbpy)PtC₂CF₃ were grown by slow evaporation from a solution of the complex in CH₂Cl₂. Single crystal X-ray diffraction data were collected at 100 K using a Bruker D8 Venture diffractometer with Mo K α radiation ($\lambda = 0.71073 \text{ Å}$) from a microfocus source, and a Photon 2 detector. Data collection, data processing (SAINT), scaling, and absorption correction (SADABS, multi-scan) were performed using the Apex 3 software suite.⁶² Space group determination (XPREP), structure solution by intrinsic phasing (SHELXT), and structure refinement by full-matrix least squares techniques on F^2 (SHELXL) were performed using the SHELXTL software package.⁶³ All non-hydrogen atoms were refined anisotropically. Hydrogen atoms attached to carbon atoms were placed in calculated positions using appropriate riding models, with $U_{\rm eq}$ of the hydrogen atoms set to 1.2 times that of their parent carbon atoms. Further details of the refinement and crystallographic data are given in the Supporting Information and are available through the Cambridge Crystallographic Data Centre, CCDC deposition number 2167216.

Syntheses. $(t^{-Bu2}bpy)Pt(C_2CF3)_2$ (1CF₃). An oven-dried, two-neck round-bottom flask (25 mL) under a positive pressure of Ar was charged with (t-Bu2bpy)PtCl₂ (50 mg, 0.094 mmol), CuI (4 mg, cat.), and a degassed solution of dichloromethane/diisopropylamine (3:1, v/v, 8 mL) and stirred. The flask was then charged with 3,3,3trifluoropropyne (15 mL, 0.62 mmol) using a syringe through a septum. Upon addition of HC≡CCF₃ (g), the connection to the Ar manifold was replaced with an Ar-filled balloon (attached via a short cannula). After 18 h of stirring, the resulting yellow solid was filtered and washed with hexanes $(1 \times 10 \text{ mL})$ and water $(1 \times 10 \text{ mL})$ and dried under vacuum. No further purification was performed. Yield: 0.037 g (0.057 mmol, 61%). Anal. Calcd for PtC₂₄H₂₄N₂F₆: H, 3.72; C, 44.38; N, 4.31. Found: H, 3.74; C, 44.02; N, 4.35%. ¹H NMR (400 MHz, CD₂Cl₂): δ 9.23 (dd, $J_{\rm H-H}$ = 6.0, 0.6 Hz, 2H); 8.04 (d, $J_{\rm H-H}$ = 1.9 Hz, 2H); 7.67 (dd, 2H, J_{H-H} = 6.0, 2.0 Hz, 2H); 1.45 (s, 12H). UV-vis (CH₂Cl₂): $\lambda_{\text{max}}/\text{nm}$ (ε/dm^3 mol⁻¹ cm⁻¹) 354 (6190), 319 (15,900), 306 (12,600).

 $(^{Ph2}bpy)Pt(C_2CF_3)_2$ (**2CF**₃). The procedure for the synthesis of 1CF₃ was followed using $(^{Ph2}bpy)PtCl_2$ (49 mg, 0.085 mmol), CuI (6 mg, cat.), dichloromethane/diisopropylamine (3:1, v/v, 8 mL), and HC≡ CCF₃ (g) (20 mL, 0.83 mmol). After 6.5 h, an additional supply of HC≡CCF₃ (15 mL, 2.50 mmol) was injected after thin-layer chromatography indicated incomplete reaction, and the reaction was allowed to proceed for an additional 18 h at room temperature. The resulting yellow solid was filtered and washed with hexanes (1 × 10 mL). Purification by column chromatography (SiO₂, 2.5 cm × 7 cm, dry load) was performed using dichloromethane as the eluent (R_f = 0.83). Yield: 0.039 g (0.057 mmol, 67%). Anal. Calcd for PtC₂₈H₁₆N₂F₆·1/2H₂O: H, 2.45; C, 48.15; N, 4.01. Found: H, 2.45; C, 48.14; N, 3.92%. ¹H NMR (400 MHz, DMSO- d_6): δ 9.22 (d, J_{H-H} = 2.0 Hz, 2H); 9.15 (dd, J_{H-H} = 6.0, 0.5 Hz, 2H); 8.36 (dd, J_{H-H} = 6.0, 2.0 Hz, 2H); 8.16 (dd, J_{H-H} = 7.2, 2.5 Hz, 4H); 7.66 (m, 6H). UV−vis (CH₂Cl₂): λ_{max}/mm (ε/dm^3 mol⁻¹ cm⁻¹) 363 (11,100), 332 (18,700), 315 (17,000).

(phbpy)PtC₂CF₃ (3CF₃). The procedure for the synthesis of 1CF₃ was followed using (phbpy)PtCl (33 mg, 0.072 mmol), CuI (5 mg, cat.), dichloromethane/diisopropylamine (3:1, v/v, 8 mL), and HC≡ CCF₃ gas (12 mL, 0.50 mmol). After 24 h, the resulting red solid was filtered and washed with diethyl ether (1 × 5 mL) and dried under vacuum. No further purification was performed. Yield: 0.026 g (0.050 mmol, 70%). Anal. Calcd for PtC₁₉H₁₁N₂F₃·1/2H₂O: H, 2.28; C, 43.19; N, 5.30. Found: H, 2.29; C, 43.19; N, 5.31%. ¹H NMR (500 MHz, DMSO- d_6): δ 8.75 (dd, J_{H-H} = 5.3, 1.6 Hz, 1H), 8.47 (d, J_{H-H} = 7.8 Hz, 1H), 8.32 (td, J_{H-H} = 7.8, 1.6 Hz, 1H), 8.19 (d, J_{H-H} = 7.9 Hz, 1H), 8.10 (t, J_{H-H} = 8.0 Hz, 1H), 7.99 (d, J_{H-H} = 8.0 Hz, 1H), 7.84 (ddd, J_{H-H} = 7.8, 5.2, 1.3 Hz, 1H), 7.60 (dd, J_{H-H} = 7.6, 1.6 Hz, 1H), 7.46 (dd, $J_{\rm H-H}$ = 7.3, 1.4 Hz, 1H), 7.10 (td, $J_{\rm H-H}$ = 7.4, 1.6 Hz, 1H), 7.05 (td, $J_{\rm H-H}$ = 7.5, 1.4 Hz, 1H). ¹³C NMR (125 MHz, DMSO d_6 , vs ¹³C solvent δ 39.52): δ 164.03, 157.37, 154.55, 150.89, 147.19, 141.18, 140.76, 140.64, 136.90, 131.06, 128.97, 125.35, 124.47, 124.31, 119.66 ($J_{\rm C-F}$ = 12 Hz), 115.41, 113.37, 88.48 ($J_{\rm C-F}$ = 43 Hz). UV-vis (CH₂Cl₂): $\lambda_{\rm max}/{\rm nm}~(\varepsilon/{\rm dm}^3~{\rm mol}^{-1}~{\rm cm}^{-1})$ 361 (9280), 327 (12,400).

■ RESULTS AND DISCUSSION

Syntheses. Each complex was synthesized by modified literature procedures derived by Sonogashira *et al.*^{23,64,65} The corresponding LPtCl_x, (^{t-Bu2}bpy)PtCl₂, (^{Ph2}bpy)PtCl₂, or (phbpy)PtCl was treated with 3,3,3-trifluoropropyne gas in dichloromethane/diisopropylamine solvent in the presence of a CuI catalyst (Figure 3). Two of the complexes, **1CF**₃ and

Figure 3. General synthetic scheme for the synthesis of the Pt trifluoropropynyl complexes.

 3CF_3 , precipitated from solution as analytically pure solids, whereas 2CF_3 required purification by column chromatography, following separation from the reaction mixture. All complexes are air-stable and photostable in the solid state and in solution. Both 1CF_3 (2.9 \times 10^{-4} M) and 2CF_3 (3.3 \times 10^{-3} M) are sparingly soluble in CH_2Cl_2 but insoluble in other organic solvents, whereas 3CF_3 is soluble in toluene and DMSO, in addition to being slightly soluble in CH_2Cl_2 (2.5 \times 10^{-3} M).

Crystallography. Crystals of $3CF_3$ suitable for X-ray diffraction were grown by slow evaporation of a CH_2Cl_2 solution. We were unable to grow single crystals suitable for

diffraction for 1CF₃ and 2CF₃. The crystal structure of 3CF₃ presents a distorted square-planar environment around Pt (Figure 4, Table S1). The long-range structure involves stacks

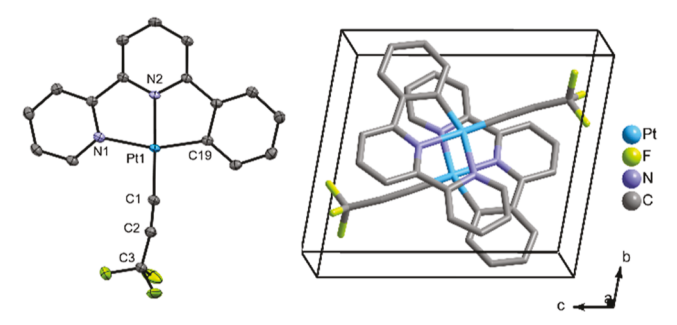


Figure 4. Structure of $3CF_3$ shown as 50% probability ellipsoids (left) and stacked (phbpy)PtC₂CF₃ complexes within the unit cell viewed slightly off the a-axis (right). Hydrogen atoms are omitted for clarity. Key interatomic distances: Pt(1)-C(1) 1.954(2) Å; Pt(1)-C(19) 1.996(2) Å; Pt(1)-N(1) 2.1147(18) Å; Pt(1)-N(2) 1.9923(18) Å; Pt(1)···Pt(2) 3.1964(2) Å. Key interatomic angles: N(1)-Pt(1)-N(2) 78.74(7)°; C(1)-Pt(1)-C(19) 98.94(9)°; N(1)-Pt(1)-C(1) 96.91(6)°; N(2)-Pt(1)-C(19) 81.81(8)°.

of complexes (stacking along the *a*-axis) alternating in their orientation because of inversion symmetry. The overlap pattern forms offset π -stacking interactions, including some involving the alkynyl carbon atom. Neighboring stacks connect through weak C–H···F interactions (Figure S4). The alkynyl ligand is slightly bent [C–C–C = 168.8(2)°]. The Pt···Pt distance of neighboring complexes along the *a*-axis is 3.1964(2) Å, which is significantly shorter than the sum of van der Waals radii (3.50 Å), ⁶⁶ suggesting a metallophillic interaction between the Pt centers. Other examples of short Pt···Pt distances in related compounds include (tpy)-PtNO₃ [3.185 Å, tpy = 2,6-bis(2-pyridyl)pyridine], (tpy)-PtBr (3.370–3.467 Å), ⁷⁰ (tpy)Pt(C₂C₆H₅) (3.346–363 Å), and (phbpy)PtCN (3.223–3.287 Å), making this one of the shortest Pt–Pt distances reported for terdentate Pt complexes.

Photophysical Characteristics. Absorption. The absorption spectra of the bipyridyl complexes, 1CF₃ and 2CF₃, in CH₂Cl₂ solution (Figure 5) each exhibit a broad absorption

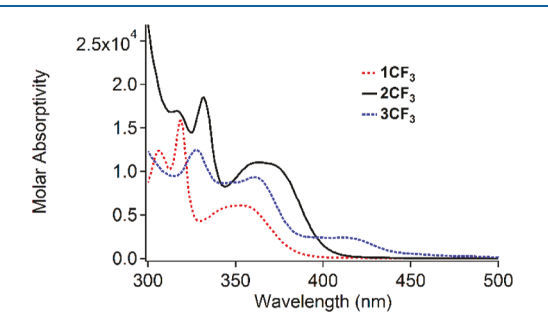


Figure 5. Overlaid UV-vis spectra in $\mathrm{CH_2Cl_2}$ solution at room temperature.

peak between 400 and 330 nm, commonly assigned to a charge-transfer transition in related alkynyl Pt diimine complexes. ^{23,32} At higher energy, peaks with well-defined vibronic progression of 1300 to 1500 cm⁻¹ are evident. Such a progression typically indicates the occurrence of a higher-energy IL (bpy) π – π * transition. ^{65,72} The absorptions of the cyclometalated 3CF₃ occur at lower energy than those of the

other two complexes (Figure 5), with the lowest-energy absorption maximum at 410 nm. The lowest-energy absorbance of (C^N^N)PtL complexes is typically assigned to 1 MLCT transitions, 32,73 and the higher-energy absorption is classified as 1 IL (bpy) $\pi-\pi^*$ transitions. 32 Data herein suggest that the lowest-energy singlet ES for 3CF₃ is not of MLCT origin but rather of phbpy ILCT (phenyl to bipyridine) character (*vide infra*). Lastly, Beer's law plots for each complex are linear, suggesting that no ground-state aggregation occurs in solution (Figure S5).

Emission. All complexes are photoluminescent in room-temperature CH₂Cl₂ solution (Figure 6, Table 1), and the

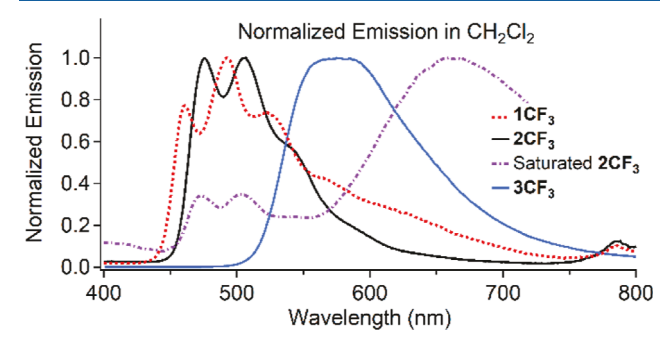


Figure 6. Normalized emission spectra in room temperature CH₂Cl₂ solution. **1**CF₃ $\lambda_{\rm ex} = 350$ [Pt] = 1×10^{-5} M; **2**CF₃ $\lambda_{\rm ex} = 350$ [Pt] = 3.5×10^{-5} M (dilute), [Pt] = 3.3×10^{-3} M (saturated); **3**CF₃, $\lambda_{\rm ex} = 361$ nm [Pt] = 2.5×10^{-4} M.

excitation spectra match the corresponding absorption spectra, indicating that emission is not due to an impurity (Figure S6). Complexes 1CF3 and 2CF3 exhibit structured emission with vibronic spacings between 1300 and 1500 cm⁻¹, which coincide with vibrational frequencies of bipyridine. The emission spectrum of the analogous dicyano complex, (t-Bu2bpy)Pt(CN)₂, is remarkably similar in energy and vibronic progression. 72,74 This vibronic progression is interpreted as emission from an IL (bpy) ${}^{3}\pi-\pi^{*}$ ES.^{2,65,72,75} At concentrations above approximately 5×10^{-5} M, the two bipyridyl complexes, 1CF₃ and 2CF₃, exhibit a broad, lowenergy emission peak (Figures 6 and S7). Such a feature is common for emissive square-planar Pt complexes and is typically ascribed to phosphorescence from an excimer formed from Pt–Pt and/or π – π interactions. ^{72–79} Lastly, the similarity between the emission spectra of 1CF3 and the analogous dicyano complex suggests that the cyano and trifluoropropynyl ligands confer remarkably similar electronic properties. Such similarities have previously been observed for complexes of Cr^{III}, Co^{III}, and Rh^{III}. 80 The addition of Pt^{II} to this list suggests that this similarity can be generalized across a range of electronic configurations.

Relative to the analogous pentafluorophenylethynyl complex, $1C_6F_5$, 23 the room-temperature, fluid-solution emission maximum of $1CF_3$ is slightly blue-shifted (501 vs 492 nm). Furthermore, the emission spectrum of the pentafluorophenylethynyl complex, $1C_6F_5$, is broad and structureless, consistent with CT-based emission. The blue shift in emission and fine structure of $1CF_3$ suggest that the energy of the MLCT and LL'CT transitions in $1CF_3$ lies above the IL π - π * (bpy) ES, whereas for the lower-energy structureless emission of $1C_6F_5$, the CT states lie below the IL π - π * (bpy) ES. This is consistent with trifluoropropynyl being a more electron-

Table 1. Photophysical Measurements of the Pt Trifluoropropynyl Complexes

		$\lambda_{\rm em} (nm)^a$		τ		$\Phi_{ ext{PL}}$	$E_{\rm a}$ (kJ/mol)	rate constants of deactivation	
		RT^b	77 K ^c	RT ^b	77 K ^c	CH ₂ Cl ₂	CH ₂ Cl ₂	$k_{\rm r} \ ({\rm s}^{-1})$	$k_{\rm nr} \ ({\rm s}^{-1})$
Soln	1CF ₃	461	449	124 ns ^d	15.4 μs	0.007	37	5.7×10^4	8.0×10^{6}
	2CF ₃	476	462	186 ns ^d	$12.1~\mu s$	0.012	26	6.5×10^4	5.3×10^{6}
	3CF ₃	570	519	1.48 μs ^e	$8.72~\mu s$	0.035	10 (12) ^f	2.4×10^{4}	6.5×10^{5}
PMMA	1CF ₃	459		10.7 μ s	13.3 μs	g	h	g	g
	2CF ₃	470		9.43 μs	$11.7~\mu s$	0.42	h	4.5×10^{4}	6.2×10^{4}
	3CF ₃	566		5.10 μs	8.8 μs	0.25	h	4.9×10^{4}	1.5×10^{5}

^aFor structured emission, the 0−0 peak is reported. For unstructured emission, the emission maximum is reported. ^bSolution data in CH₂Cl₂. ^cSolvent glass of 1:1 CH₂Cl₂ and 2-methyltetrahydrofuran (2-MeTHF). ^dExtrapolated from the Arrhenius plots of photoluminescence decay rate constants. ^eSolution purged with Ar (g). ^fIn toluene solution. ^gCould not be determined due to poor solubility and low doping percentage. ^hSee text.

Table 2. Emission Wavelength, TDDFT-Calculated $S_0 \rightarrow T_1$ Wavelength, and Population Analysis^a

	λ_{em} Soln (77 K)	T_1 (nm)	Pt	Rbpy ^b	$C_6H_4^-$	C_2R
1CF ₃	461 (449)	430	$18 \rightarrow 4 \ (-14)$	$58 \to 93 \ (35)$		$24 \rightarrow 3 \ (-21)$
2CF ₃	476 (462)	468	$25 \rightarrow 4 \ (-21)$	$48 \to 94 (46)$		$27 \rightarrow 3 \ (-24)$
3CF ₃	570 (519)	523	$28 \rightarrow 5 \ (-23)$	$17 \rightarrow 87 (70)$	$55 \rightarrow 5 \ (-50)$	$0 \to 3 \ (3)$
$1C_6F_5$	501 (450) ^c	496	$20 \rightarrow 4 \ (-16)$	$6 \rightarrow 82 \ (76)$		$74 \to 14 \ (-60)$
$3C_6F_5$	$560 (531)^d$	524	$30 \rightarrow 6 \ (-24)$	$16 \rightarrow 88 \ (72)$	$54 \rightarrow 4 \ (-50)$	$0 \to 2 \ (2)$

^aTDDFT and Mulliken population analysis used the B3LYP/6-31G(d)/LANL2DZ computational model. All structures were optimized as singlets with the B3LYP/LANL2DZ computational model. ^bPopulations presented in this column represent the sum of all atoms of the ^{t-Bu2}bpy and ^{Ph2}bpy ligand, but only the bpy portion of the phbpy ligand. ^cData from ref 23. ^dData from ref 32.

withdrawing ligand than pentafluorophenyl, as suggested by previous electrochemical experiments. In 77 K glass, the emission spectrum of $\mathbf{1C_6F_5}^{23}$ shows nearly identical vibronic spacing (1350 cm⁻¹) and essentially identical 0–0 band energies (450 nm and 449 nm respectively) as $\mathbf{1CF_3}$. The change from structureless (RT solution) to structured (77 K glass) emission in $\mathbf{1C_6F_5}$ could be explained by a change in the lowest-energy triplet state between sample media. Recall that upon incorporation into rigid medium, a CT ES will be blueshifted by a greater degree than an IL π – π * ES. He is could result in the CT ES in $\mathbf{1C_6F_5}$ being elevated above the IL π – π * ES due to the rigidity of the 77 K matrix. Lastly, because the energy of IL π – π * ESs is not significantly impacted by the electronic nature of the ancillary ligand, this would explain why the 77 K emission energies of $\mathbf{1CF_3}$ and $\mathbf{1C_6F_5}$ are very similar.

For the cyclometallated phbpy complex, 3CF₃, the roomtemperature CH₂Cl₂ emission profile is broad and structureless (Figure 6), which in related (N^N^C)Pt complexes is ascribed to a CT ES.^{32,34} The integrated emission intensity of 3CF₃ increases by a factor of 3 in deaerated solvent (Figure S8), indicating oxygen quenching, whereas the emission intensities of 1CF₃ and 2CF₃ are not diminished in air-saturated solutions at room temperature. The solution (CH₂Cl₂) emission spectrum of $3C_6F_5^{32}$ is remarkably similar to that of $3CF_3$ in both energy and shape. The 77 K emission spectra of both complexes are structured, with a vibronic spacing between 1250 and 1450 cm⁻¹. The 77 K emission of 3CF₃ is slightly blue-shifted relative to 3C₆F₅ (519 vs 531 nm). The strong similarity in emission spectra between 3CF₃ and 3C₆F₅ is more consistent with emission from a phbpy ILCT (phenyl to bipyridine) than either MLCT or LL'CT as these latter CT transitions would be significantly more impacted by the ewithdrawing character of the alkyne. The computational chemistry (vide infra) supports this conclusion.

Computational Investigation. To further investigate the nature of the emissive ESs, TDDFT experiments were

performed. Vertical $S_0 \rightarrow T_1$ absorption energies are considered good models for 0-0 transitions, especially in rigid medium where structural relaxation has little effect on the emission energy.^{81,82} A recent review demonstrated that geometry optimization using B3LYP/LANL2DZ followed by TDDFT using the functional B3LYP yielded $S_0 \rightarrow T_1$ transitions that best agreed with emission energies of Pt and Ir phosphors.⁸³ A study by the Yersin group demonstrated that the functional B3LYP also yielded balanced treatment of LC and MLCT ESs in Pt phosphors.81 Our benchmarking experiments demonstrated that for this set of complexes, TDDFT experiments using the B3LYP/6-31G(d)/LANL2DZ-(for Pt) model agreed well with emission energies and provided balanced treatment of the ES orbital character. Thus, computational modeling was performed using B3LYP/6-31G(d)/LANL2DZ//B3LYP/LANL2DZ (TDDFT//opt). All calculations employed a Tomasi-polarizable continuum model⁸⁴ assigned the dielectric constant for THF. Although the 77 K emission data were recorded in a frozen 1:1 (v/v) CH₂Cl₂/2-MeTHF matrix, TDDFT showed no meaningful difference in ES energies modeled with THF or CH2Cl2, which is not surprising, given the similar dielectric constants for these two solvents.

The population analysis and MO images (Table 2, Figure 7) associated with the $S_0 \rightarrow T_1$ transitions are in good agreement with the experimental characterization of these ESs. For example, the lowest-energy triplet transition of 1CF₃ is composed of equal parts $H-4 \rightarrow LUMO$ and $HOMO \rightarrow LUMO$, representing IL (bpy) $\pi-\pi^*$ and MLCT/LL'CT transitions, respectively. Population analysis (Table 2) supports these observations, indicating a greater degree of IL (bpy) character than CT character. A very similar transition character is observed in the computational data for 2CF₃ (Chart S2). By contrast, the $S_0 \rightarrow T_1$ transition of the pentafluorophenylethynyl complex, $1C_6F_5$, displays almost

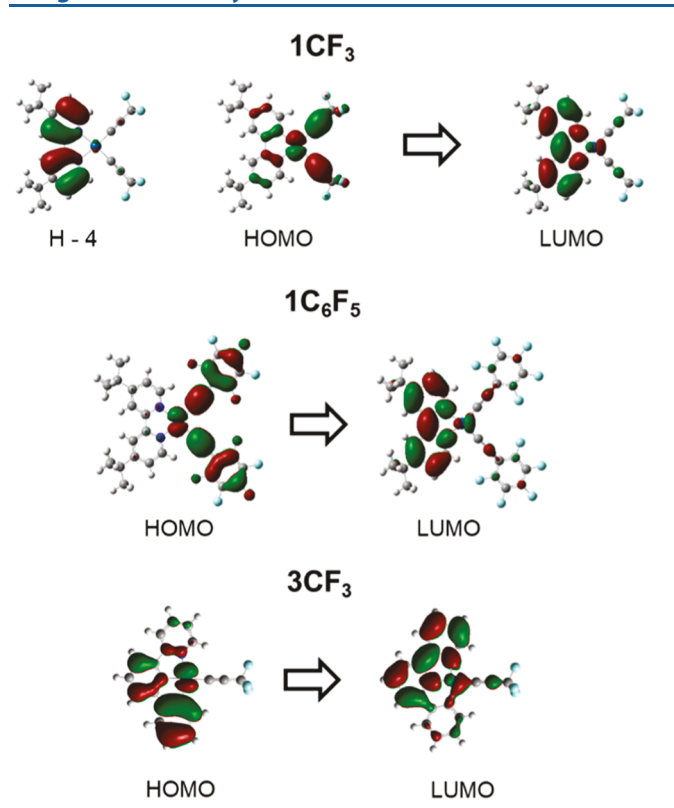


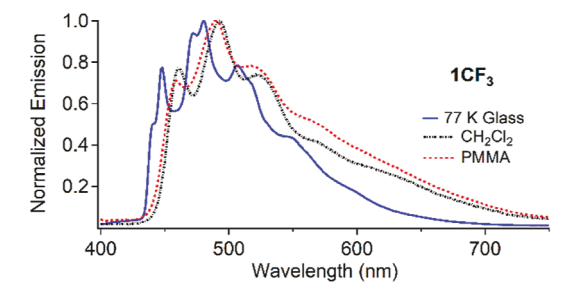
Figure 7. Key orbital images associated with the $S_0 \rightarrow T_1$ transition.

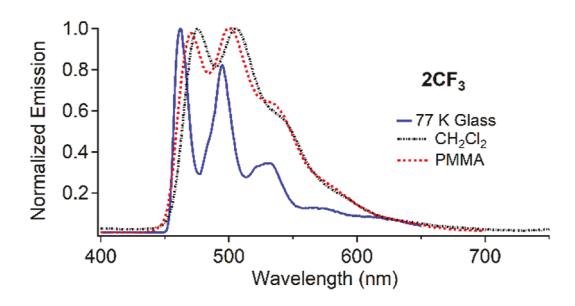
entirely HOMO →LUMO transition, with only MLCT/LL'CT character observed (Table 2, Figure 7).

TDDFT analysis of 3CF₃ suggests that the lowest-energy triplet and singlet ES are composed almost entirely of HOMO → LUMO character (Figure 7, Chart S3). Orbital images suggest that the lowest-energy triplet and singlet ES of 3CF₃ and 3C₆F₅ (Chart S7) are mostly of phbpy ILCT (phenyl to bipyridyl) character. The population analysis supports this conclusion and reveals a nontrivial amount of MLCT character in the transition, which explains the slight blue shift in 77 K emission from 3C₆F₅ to 3CF₃. The model predicts nearly identical character and emission energy for 3CF₃ and 3C₆F₅, which is in agreement with the experimental data. As indicated above, this similarity is likely because the ancillary ligand has little effect on the Ph \rightarrow bpy CT transition. In conclusion, one key impact of the trifluoropropynyl ligand is that it elevates the energy of the MLCT and LL'CT ES above that of the IL π – π * ES, making it a useful co-ligand when IL emission is desired.

Effect of PMMA. It is well documented that incorporation into PMMA films often increases Φ_{PL} and ES lifetimes and blue-shifts emission energies, and the extent of these effects depends on the degree of distortion of the ESs involved in both the emission and the nonradiative decay. ^{18,28,43–46,85} The two bipyridyl complexes, 1CF₃ and 2CF₃, exhibit smaller rigidochromic shifts between solution and PMMA than 3CF₃ (Figure 8), which is consistent with the IL $\pi-\pi^*$ ES character assignment of the 1CF₃ and 2CF₃ complexes and the MLCT/ILCT character of 3CF₃, the former being less distorted than the latter.

Complexes $1CF_3$ and $2CF_3$ are visibly more emissive under UV-lamp excitation in room temperature PMMA film than in solution, with ES lifetimes increasing by approximately 2 orders of magnitude (Table 1, Figures S9–S11). Furthermore, Φ_{PL} for $2CF_3$ increases by a factor of 35 in PMMA film. Rate





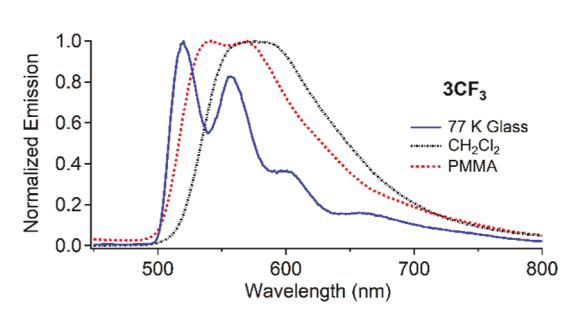


Figure 8. Normalized emission spectra of 1CF_3 [Pt] = 1×10^{-5} M (CH₂Cl₂); $\lambda_{\text{ex}} = 350$ (CH₂Cl₂ solution and PMMA), $\lambda_{\text{ex}} = 354$ (77 K); PMMA film made by spin coating. 2CF_3 [Pt] = 3.5×10^{-5} M (CH₂Cl₂); $\lambda_{\text{ex}} = 360$ nm (PMMA and 77 K), $\lambda_{\text{ex}} = 350$ (CH₂Cl₂); PMMA film made by doctor blading. 3CF_3 [Pt] = 2.5×10^{-4} M (CH₂Cl₂); $\lambda_{\text{ex}} = 361$ nm; PMMA film made by spin coating.

constants for radiative $(k_{\rm r})$ and nonradiative $(k_{\rm nr})$ relaxation (Table 1) from the emissive ES were determined from the overall rate constant for ES deactivation $(k_{\rm d})$ and $\Phi_{\rm PL}$, using eqs 1 and 2. Incorporation into PMMA film decreases $k_{\rm nr}$

$$\Phi_{\rm PL} = \frac{k_{\rm r}}{k_{\rm d}} \tag{1}$$

$$k_{\rm d} = k_{\rm r} + k_{\rm nr} \tag{2}$$

by a factor of 85 in $2CF_3$, while the radiative rate constant, k_r , is relatively unchanged, indicating that rigidoluminescence is dominated by slowing the nonradiative pathway. Though Φ_{PL} of $1CF_3$ was not measured in PMMA (due to low dopant concentration owing to low solubility), the similar degrees of ES lifetime elongation in PMMA film (Table 1) and the structural and spectroscopic similarities between $1CF_3$ and $2CF_3$ suggest qualitatively similar behavior.

For 3CF_3 , the approximately one order of magnitude increase in Φ_{PL} upon incorporation into PMMA film is due to both a twofold increase in k_{r} and a fourfold decrease in k_{nr} , a significantly smaller decrease in k_{nr} than for 2CF_3 . One explanation for the smaller impact of rigidification on k_{nr} in 3CF_3 is that the terdentate complex, being inherently more rigid, is less susceptible to ES distortions that stabilize the ^3MC

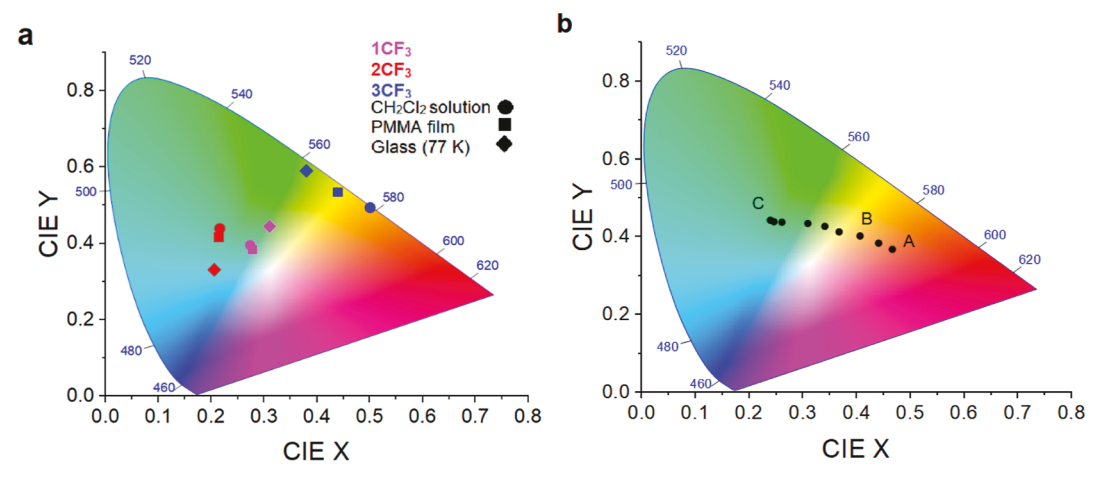


Figure 9. (a) Chromaticity of emission of the three trifluoropropynyl complexes in CH_2Cl_2 solution, PMMA film, and 77 K glass. CIE coordinates $1CF_3$ CH_2Cl_2 (0.274, 0.396), PMMA (0.254, 0.396), 77 K (0.310, 0.445); $2CF_3$ CH_2Cl_2 (0.216, 0.439), PMMA (0.212, 0.395), 77 K (0.206, 0.331); $3CF_3$ CH_2Cl_2 (0.501, 0.494), PMMA (0.478, 0.515), 77 K (0.380, 0.590) based on CIE 1931 2°. (b) Chromaticity of emission of $2CF_3$ in CH_2Cl_2 solution across concentrations ranging from saturated (A, 3.3 × 10^{-3} M) to dilute (C, 1×10^{-5} M).

state, reducing the impact of medium effects on rigid-oluminescence. ^13 The long-lived luminescence and high $\Phi_{\rm PL}$ of 3CF $_3$ in solution (cf. 1CF $_3$ and 2CF $_3$) (Table 1) are consistent with 3CF $_3$ being inherently more rigid.

For the complexes investigated herein, another explanation for the rigidoluminescence behavior is a lack of diffusion-mediated self-quenching in PMMA film. However, plots of integrated photoluminescence intensity *versus* the concentration for each compound in CH₂Cl₂ are linear over concentrations at which solution lifetimes were measured, indicating a lack of self-quenching behavior (Figure S12).

To probe the mechanism of nonradiative relaxation, activation barriers associated with solution phase ES relaxation for 1CF_3 , 2CF_3 , and 3CF_3 were determined from Arrhenius plots for the rate constants for ES deactivation (Figures S13 and S14). The energy barriers associated with deactivation of T_1 in solution for 1CF_3 , 2CF_3 , and 3CF_3 were determined to be 37, 26, and 10 kJ/mol, respectively (Table 1). These are similar in magnitude to those determined for Pt^{II} NHC complexes¹⁶ and Ru^{II} polypyridyl complexes,⁸⁶ where thermal access of the ^3MC state was invoked.

In PMMA, Arrhenius plots for 1CF_3 and 2CF_3 are very flat over the accessible temperature range of the cuvette holder (-28.5 to +105 °C), likely indicating this to be below the temperature dependent region (Figures S15–S17). The Arrhenius plot for 1CF_3 is slightly curved, perhaps indicating a transition into thermally activated behavior or softening of the PMMA. As a result, activation barriers could not be determined for PMMA samples, and experimental E_a values between the two media could not be directly compared.

Because experimental $E_{\rm a}$ values could not be measured for PMMA film, TDDFT-predicted transition energies were used to estimate the energy gap between the emissive state and the 3 MC state in these rigid systems since TDDFT is based on vertical transitions at the GS geometry. The lowest-energy 3 MC states were identified for all three complexes by screening triplet states for high degrees of d-d transition character (Charts S1-S3). The ES activation barrier was estimated as the difference between the lowest-energy 3 MC state and the lowest-energy triplet state (3 MC-T $_1$), resulting in values of approximately 150 kJ/mol for 1CF $_3$, 170 kJ/mol for 2CF $_3$, and 190 kJ/mol for 3CF $_3$, which are in typical ranges for TDDFT-

calculated T_1 – 3 MC energy differences in Pt phosphors. ^{87,88} If TDDFT is considered representative of the more rigid film environment, then these larger values in E_a support the hypothesis that the deactivating 3 MC is stabilized by M–L bond distortions allowed in the solution state.

Emission Chromaticity. Due to rigidochromic shifts, the color of monomer emission for each complex differs between environments (dilute CH2Cl2, 77 K glass, and PMMA film, Figure 9a). In addition, the low-energy excimer emission of 1CF₃ and 2CF₃ increases in intensity with increasing concentration. As a result, the emission color can be tuned by varying the concentration (Figure 9b). At high concentrations, the excimer emission dominates the spectrum, resulting in yellow (1CF₃) or orange (2CF₃) emission. At very dilute concentrations, excimer emission is almost entirely absent, enabling the blue-cyan emission of the pure monomer. Interestingly, at 8.40×10^{-4} M in CH₂Cl₂, 2CF₃ exhibits warm white emission with CIE (0.4062, 0.4023) (Figure 9b point B), which is close to CIE standard illuminant "F3, fluorescent white" (0.4091, 0.3941). Single-component white emission is desired for white OLEDs (WOLEDs).3,89-91 However, upon incorporation into PMMA, monomer emission dominates up to the solubility limit for solution (CH₂Cl₂) processing of the film (0.15 wt % for 1CF₃ and 1.8 wt % for 2CF₃). In fact, CH₂Cl₂/PMMA solutions of 1CF₃ and 2CF₃ that show significant excimer emission show no evidence of the excimer emission upon curing (Figures 10 and S17). This is likely because excimer emission requires diffusion at these low concentrations 78,79,92 and because Φ_{PL} for monomer emission increases drastically in PMMA film. Furthermore, below the solubility limit, the emission spectra and lifetimes in PMMA film are independent of the dopant concentration (0.04 to 1.8 wt %), as demonstrated for 2CF₃ (Figure S18). Several examples of single-component white emission for WOLEDs involve excimer emission of Pt complexes, but each case required concentrations upward of 10 wt % [Pt], and typically utilized vapor deposition^{3,89,92} instead of solution processing. Due to the poor solubilities of 1CF₃ and 2CF₃, it is not likely that solution-processed single-component white emitting films can be prepared from the complexes of this study.

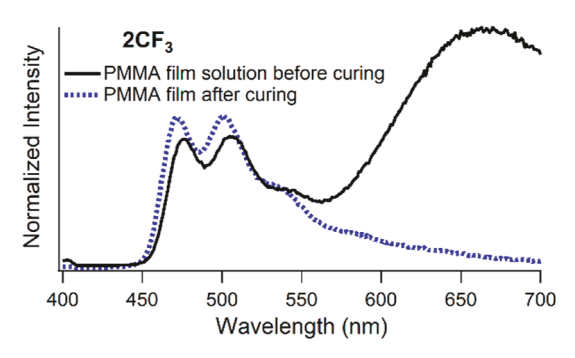


Figure 10. Emission spectrum of $2CF_3$ (3.3 \times 10⁻³ M) in CH_2Cl_2 solution containing PMMA before curing and the resulting PMMA film after curing.

CONCLUSIONS AND OUTLOOK

Though the trifluoropropynyl ligand had previously been demonstrated to be a stronger-field ligand and more electronwithdrawing than the pentafluorophenylethynyl ligand, there have been no investigations regarding the impact that this would have on the emission from complexes with MLCT and LL'CT emissive states. Herein, we demonstrate that for a series of substituted bipyridyl complexes, the emissive states are almost entirely IL in character. This is likely due to the electron-poor nature of the trifluoropropynyl ligand raising the energy of the MLCT and LL'CT states above that of the IL states. For this class of complexes, this suggests that a limit has been reached, where further blue-shifting of emission will require ligands with higher-energy IL states. Such a strategy has already been demonstrated by the Schanze group in Pt butadiynyl complexes, where the emissive state is of $\pi - \pi^*$ (butadiyne) character, resulting in high color-purity, deep-blue emission. 18 Similar studies have suggested using ligands with smaller π -conjugated systems to blue-shift π - π * emission energies in Ir pyridyl compounds. 14 Thus, trifluoropropynyl may serve as a useful co-ligand in cases where IL emission is desirable.

Furthermore, this work adds to the growing body of literature demonstrating the profound impact that environmental rigidification can have on the emission quantum yield. Thus, it is worthwhile to augment investigations of emissive complexes with characterization in rigid environments, particularly for complexes with low emission quantum yields. With respect to the Pt complexes investigated herein, the data are consistent with a mechanism for rigidoluminescence wherein the rigid environment raises the energy of the ³MC states, rendering them thermally inaccessible. Lastly, in addition to increasing Φ_{PL} , the PMMA environment diminishes excimer emission, presumably because diffusional collision between an excited- and ground-state monomer is prevented. As a consequence, achieving white emission from a mixture of monomer and excimer emission in a rigid environment should require much higher chromophore concentrations, such that the film contains an appropriate fraction of pre-organized chromophore pairs required for excimer emission.

ASSOCIATED CONTENT

Supporting Information

The Supporting Information is available free of charge at https://pubs.acs.org/doi/10.1021/acs.inorgchem.2c01564.

 1H NMR for all complexes and ^{13}C NMR for 3CF $_3$; FTIR spectra for all complexes; crystallographic data for 3CF $_3$ and packing arrangement for the structure; Beer's law plots and excitation spectra for all complexes; emission spectrum of 1CF $_3$ in saturated solution; emission spectra of 3CF $_3$ in air-saturated CH $_2$ Cl $_2$ and in Ar-purged solvent; computational benchmarking results; luminescence decay traces for ES lifetime determination; plots used to calculate the solution phase relative $\Phi_{\rm PL}$; Arrhenius plots for ES deactivation; emission of 1CF $_3$ and 2CF $_3$ in PMMA before and after curing; emission spectra of 2CF $_3$ in PMMA films of different dopant concentrations; TDDFT data and molecular orbital images (PDF)

Cartesian coordinates for all optimized structures as singlets in dichloromethane at the B3LYP/LANL2DZ level (XYZ)

Accession Codes

CCDC 2167216 contains the supplementary crystallographic data for this paper. These data can be obtained free of charge via www.ccdc.cam.ac.uk/data_request/cif, or by emailing data_request@ccdc.cam.ac.uk, or by contacting The Cambridge Crystallographic Data Centre, 12 Union Road, Cambridge CB2 1EZ, UK; fax: +44 1223 336033.

AUTHOR INFORMATION

Corresponding Author

Paul S. Wagenknecht — Department of Chemistry, Furman University, Greenville, South Carolina 29609, United States; orcid.org/0000-0001-8698-073X; Email: paul.wagenknecht@furman.edu

Authors

Jackson S. McCarthy — Department of Chemistry, Furman University, Greenville, South Carolina 29609, United States Mary Jo McCormick — Department of Chemistry, Furman University, Greenville, South Carolina 29609, United States John H. Zimmerman — Department of Chemistry, Furman University, Greenville, South Carolina 29609, United States H. Rhodes Hambrick — Department of Chemistry, Furman University, Greenville, South Carolina 29609, United States Wilson M. Thomas — Department of Chemistry, Furman University, Greenville, South Carolina 29609, United States Colin D. McMillen — Department of Chemistry, Clemson University, Clemson, South Carolina 29634, United States; orcid.org/0000-0002-7773-8797

Complete contact information is available at: https://pubs.acs.org/10.1021/acs.inorgchem.2c01564

Note:

The authors declare no competing financial interest.

ACKNOWLEDGMENTS

This material is based upon work supported by the National Science Foundation under grant no. 2055326 and through the EPSCoR Program under NSF Award no. OIA-1655740. Any opinions, findings, and conclusions or recommendations expressed in this material are those of the authors and do not necessarily reflect those of the National Science Foundation. M.J.M. and J.H.Z. acknowledge support from the Furman Summer Fellows Program. The authors thank George C. Shields for providing computational infrastructure,

in part through a Research Corporation for Science Advancement Cottrell Instrumentation Supplements Award #27446.

REFERENCES

- (1) Thompson, M. E.; Djurovich, P. E.; Barlow, S.; Marder, S. In *Comprehensive Organometallic Chemistry*; O'Hare, D., Ed.; Elsevier: Oxford, 2007; Vol. 12, p 101.
- (2) Brooks, J.; Babayan, Y.; Lamansky, S.; Djurovich, P. I.; Tsyba, I.; Bau, R.; Thompson, M. E. Synthesis and Characterization of Phosphorescent Cyclometalated Platinum Complexes. *Inorg. Chem.* **2002**, *41*, 3055–3066.
- (3) Adamovich, V.; Brooks, J.; Tamayo, A.; Alexander, A. M.; Djurovich, P. I.; D'Andrade, B. W.; Adachi, C.; Forrest, S. R.; Thompson, M. E. High efficiency single dopant white electrophosphorescent light emitting diodes. *New J. Chem.* **2002**, *26*, 1171–1178.
- (4) Zhang, J.; Wang, L.; Zhong, A.; Huang, G.; Wu, F.; Li, D.; Teng, M.; Wang, J.; Han, D. Deep red PhOLED from dimeric salophen Platinum(II) complexes. *Dyes Pigm.* **2019**, *162*, 590–598.
- (5) Marian, C. M. Understanding and Controlling Intersystem Crossing in Molecules. *Annu. Rev. Phys. Chem.* **2021**, 72, 617–640.
- (6) Sasikumar, D.; John, A. T.; Sunny, J.; Hariharan, M. Access to the triplet excited states of organic chromophores. *Chem. Soc. Rev.* **2020**, *49*, 6122–6140.
- (7) Gildea, L. F.; Williams, J. A. G. Iridium and platinum complexes for OLEDS. In *Organic Light-Emitting Diodes (OLEDs)*; Woodhead Publishing Series in Electronic and Optical Materials; Buckley, A., Ed.; Woodhead Publishing, 2013; pp 77–113.
- (8) Xiang, H.-F.; Lai, S.-W.; Lai, P. T.; Che, C.-M. Phosphorescent Platinum(II) Materials for OLED Applications. In *Highly Efficient OLEDs with Phosphorescent Materials*; Yersin, H., Ed.; Wiley-VCH: Weinheim, 2008; Chapter 7, pp 259–282.
- (9) Li, K.; Ming Tong, G. S.; Wan, Q.; Cheng, G.; Tong, W.-Y.; Ang, W.-H.; Kwong, W.-L.; Che, C.-M. Highly Phosphorescent Platinum-(II) Emitters: Photophysics, Materials and Biological Applications. *Chem. Sci.* **2016**, *7*, 1653–1673.
- (10) Zhu, Y.-C.; Zhou, L.; Li, H.-Y.; Xu, Q.-L.; Teng, M.-Y.; Zheng, Y.-X.; Zuo, J.-L.; Zhang, H.-J.; You, X.-Z. Highly Efficient Green and Blue-Green Phosphorescent OLEDs Based on Iridium Complexes with the Tetraphenylimidodiphosphinate Ligand. *Adv. Mater.* **2011**, 23, 4041–4046.
- (11) Li, G.; Zhu, D.; Peng, T.; Liu, Y.; Wang, Y.; Bryce, M. R. Very High Efficiency Orange-Red Light-Emitting Devices with Low Roll-Off at High Luminance Based on an Ideal Host—Guest System Consisting of Two Novel Phosphorescent Iridium Complexes with Bipolar Transport. *Adv. Funct. Mater.* **2014**, *24*, 7420—7426.
- (12) Sun, Y.; Yang, X.; Feng, Z.; Liu, B.; Zhong, D.; Zhang, J.; Zhou, G.; Wu, Z. Highly Efficient Deep-Red Organic Light-Emitting Devices Based on Asymmetric Iridium(III) Complexes with the Thianthrene 5,5,10,10-Tetraoxide Moiety. ACS Appl. Mater. Interfaces 2019, 11, 26152–26164.
- (13) Rausch, A. F.; Murphy, L.; Williams, J. A. G.; Yersin, H. Improving the performance of Pt(II) complexes for blue light emission by enhancing the molecular rigidity. *Inorg. Chem.* **2012**, *51*, 312–319.
- (14) Du, B.-S.; Liao, J.-L.; Huang, M.-H.; Lin, C.-H.; Lin, H.-W.; Chi, Y.; Pan, H.-A.; Fan, G.-L.; Wong, K.-T.; Lee, G.-H.; Chou, P.-T. Os(II) based green to red phosphors: A great prospect for solution-processed, highly efficient organic light emitting diodes. *Adv. Funct. Mater.* **2012**, 22, 3491–3499.
- (15) Wagenknecht, P. S.; Ford, P. C. Metal Centered Ligand Field Excited States: Their Roles in the Design and Performance of Transition Metal Based Photochemical Molecular Devices. *Coord. Chem. Rev.* **2011**, 255, 591–616.
- (16) Bullock, J. D.; Valandro, S. R.; Sulicz, A. N.; Zeman, C. J.; Abboud, K. A.; Schanze, K. S. Blue Phosphorescent trans-N-Heterocyclic Carbene Platinum Acetylides: Dependence on Energy Gap and Conformation. *J. Phys. Chem. A* **2019**, *123*, 9069–9078.

- (17) Williams, J. A. G. Platinum. In *Photochemistry and Photophysics of Coordination Compounds II*; Springer, 2007; pp 205–268.
- (18) He, R.; Xu, Z.; Valandro, S.; Arman, H. D.; Xue, J.; Schanze, K. S. High-Purity and Saturated Deep-Blue Luminescence from trans-NHC Platinum(II) Butadiyne Complexes: Properties and Organic Light Emitting Diode Application. ACS Appl. Mater. Interfaces 2021, 13, 5327–5337.
- (19) Fleetham, T.; Golden, J. H.; Idris, M.; Hau, H.-M.; Muthiah Ravinson, D. S.; Djurovich, P. I.; Thompson, M. E. Tuning State Energies for Narrow Blue Emission in Tetradentate Pyridyl-Carbazole Platinum Complexes. *Inorg. Chem.* **2019**, *58*, 12348–12357.
- (20) Sajoto, T.; Djurovich, P. I.; Tamayo, A.; Yousufuddin, M.; Bau, R.; Thompson, M. E.; Holmes, R. J.; Forrest, S. R. Blue and Near-UV Phosphorescence from Iridium Complexes with Cyclometalated Pyrazolyl or N-Heterocyclic Carbene Ligands. *Inorg. Chem.* **2005**, 44, 7992–8003.
- (21) Idris, M.; Kapper, S. C.; Tadle, A. C.; Batagoda, T.; Muthiah Ravinson, D. S.; Abimbola, O.; Djurovich, P. I.; Kim, J.; Coburn, C.; Forrest, S. R.; Thompson, M. E. Blue Emissive fac/mer-Iridium (III) NHC Carbene Complexes and their Application in OLEDs. *Adv. Opt. Mater.* **2021**, *9*, 2001994.
- (22) Zhang, Y.; Blacque, O.; Venkatesan, K. Highly Efficient Deep-Blue Emitters Based on Cis and Trans N-Heterocyclic Carbene Pt^{II}acetylide Complexes: Synthesis, Photophysical Properties, and Mechanistic Studies. *Chem.—Eur. J.* **2013**, *19*, 15689–15701.
- (23) Lu, W.; Chan, M. C. W.; Zhu, N.; Che, C.-M.; He, Z.; Wong, K.-Y. Structural Basis for Vapoluminescent Organoplatinum Materials Derived from Noncovalent Interactions as Recognition Components. *Chem.—Eur. J.* **2003**, *9*, 6155–6166.
- (24) Pomestchenko, I. E.; Castellano, F. N. Solvent Switching between Charge Transfer and Intraligand Excited States in a Multichromophoric Platinum(II) Complex. J. Phys. Chem. A 2004, 108, 3485–3492.
- (25) Hua, F.; Kinayyigit, S.; Cable, J. R.; Castellano, F. N. Platinum(II) Diimine Diacetylides: Metallacyclization Enhances Photophysical Properties. *Inorg. Chem.* **2006**, *45*, 4304–4306. (26) Chan, S.-C.; Chan, M. C. W.; Wang, Y.; Che, C.-M.; Cheung,
- (26) Chan, S.-C.; Chan, M. C. W.; Wang, Y.; Che, C.-M.; Cheung, K.-K.; Zhu, N. Organic Light-Emitting Materials Based on Bis-(arylacetylide)platinum(II) Complexes Bearing Substituted Bipyridine and Phenanthroline Ligands: Photo- and Electroluminescence from ³MLCT Excited States. *Chem.—Eur. J.* **2001**, *7*, 4180–4190.
- (27) Zhong, F.; Zhao, J. An NN Platinum(II) Bis(acetylide) Complex with Naphthalimideand Pyrene Ligands: Synthesis, Photophysical Properties, and Application in Triplet—Triplet Annihilation Upconversion. *Eur. J. Inorg. Chem.* **2017**, 2017, 5196—5204.
- (28) Whittle, C. E.; Weinstein, J. A.; George, M. W.; Schanze, K. S. Photophysics of Diimine Platinum(II) Bis-Acetylide Complexes. *Inorg. Chem.* **2001**, *40*, 4053–4062.
- (29) Miskowski, V. M.; Houlding, V. H. Electronic Spectra and Photophysics of Platinum(II) Complexes with α -Diimine Ligands. Solid-State Effects. 1. Monomers and Ligand π Dimers. *Inorg. Chem.* 1989, 28, 1529–1533.
- (30) Miskowski, V. M.; Houlding, V. H.; Che, C. M.; Wang, Y. Electronic Spectra and Photophysics of Platinum (II) Complexes with α -Diimine Ligands. Mixed Complexes with Halide Ligands. *Inorg. Chem.* **1993**, 32, 2518–2524.
- (31) Castellano, F. N.; Pomestchenko, I. E.; Shikhova, E.; Hua, F.; Muro, M. L.; Rajapakse, N. Photophysics I bipyridyl and terpyridyl platinum(II) acetylides. *Coord. Chem. Rev.* **2006**, 250, 1819–1828.
- (32) Lu, W.; Mi, B.-X.; Chan, M. C. W.; Hui, Z.; Che, C.-M.; Zhu, N.; Lee, S.-T. Light-Emitting Tridentate Cyclometalated Platinum(II) Complexes Containing σ -Alkynyl Auxiliaries: Tuning of Photo- and Electrophosphorescence. *J. Am. Chem. Soc.* **2004**, *126*, 4958–4971.
- (33) Sicilia, V.; Arnal, L.; Chueca, A. J.; Fuertes, S.; Babaei, A.; Igual Muñoz, A. M.; Sessolo, M.; Bolink, H. J. Highly Photoluminescent Blue Ionic Platinum-Based Emitters. *Inorg. Chem.* **2020**, *59*, 1145–1152.
- (34) Kui, S. C. F.; Sham, I. H. T.; Cheung, C. C. C.; Ma, C. W.; Yan, B.; Zhu, N.; Che, C. M.; Fu, W. F. F. Platinum(II) Complexes with π -

- Conjugated, Naphthyl-Substituted, Cyclometalated Ligands (RĈNN): Structures and Photo- and Electroluminescence. *Chem.*—*Eur. J.* **2007**, *13*, 417–435.
- (35) Chan, C.-W.; Cheng, L.-K.; Che, C.-M. Luminescent donor-acceptor platinum(II) complexes. *Coord. Chem. Rev.* **1994**, *132*, 87–97.
- (36) Yam, V. W.-W.; Law, A. S.-Y. Luminescent d8 metal complexes of platinum(II) and gold(III): From photophysics to photofunctional materials and probes. *Coord. Chem. Rev.* **2020**, *414*, 213298.
- (37) Law, A. S.-Y.; Lee, L. C.-C.; Lo, K. K.-W.; Yam, V. W.-W. Aggregation and Supramolecular Self-Assembly of Low-Energy Red Luminescent Alkynylplatinum(II) Complexes for RNA Detection, Nucleolus Imaging, and RNA Synthesis Inhibitor Screening. *J. Am. Chem. Soc.* 2021, 143, 5396–5405.
- (38) Hissler, M.; McGarrah, J. E.; Connick, W. B.; Geiger, D. K.; Cummings, S. D.; Eisenberg, R. Platinum diimine complexes: toward a molecular photochemical device. *Coord. Chem. Rev.* **2000**, 208, 115–137.
- (39) Garethwilliams, J.; Develay, S.; Rochester, D.; Murphy, L. Optimizing the luminescence of platinum(II) complexes and their application in organic light emitting devices (OLEDs). *Coord. Chem. Rev.* 2008, 252, 2596–2611.
- (40) Houlding, V. H.; Miskowski, V. M. The effects of linear chain structure on the electronic structure of Pt(II) diimine complexes. *Coord. Chem. Rev.* **1991**, *111*, 145–152.
- (41) Na, H.; Lai, P. N.; Cañada, L. M.; Teets, T. S. Photoluminescence of Cyclometalated Iridium Complexes in Poly(methyl methacrylate) Films. *Organometallics* **2018**, *37*, 3269–3277.
- (42) Congrave, D. G.; Hsu, Y.-T.; Batsanov, A. S.; Beeby, A.; Bryce, M. R. Synthesis, Diastereomer Separation, and Optoelectronic and Structural Properties of Dinuclear Cyclometalated Iridium(III) Complexes with Bridging Diarylhydrazide Ligands. *Organometallics* 2017, 36, 981–993.
- (43) Hua, F.; Kinayyigit, S.; Rachford, A. A.; Geob, S.; Cable, J. R.; Adams, C. J.; Kirschbau, K.; Pinkerton, A. A.; Castellano, F. N. Luminescent Charge-Transfer Platinum(II) Metallacycle. *Inorg. Chem.* **2007**, *46*, 8771–8783.
- (44) Chen, P.; Meyer, T. J. Medium Effects on Charge Transfer in Metal Complexes. *Chem. Rev.* **1998**, 98, 1439–1478.
- (45) Chen, P.; Meyer, T. J. Electron Transfer in Frozen Media. *Inorg. Chem.* **1996**, *35*, 5520–5524.
- (46) Kozik, M.; Sutin, N.; Winkler, J. R. Energetics and dynamics of solvent reorganization in charge-transfer excited states. *Coord. Chem. Rev.* **1990**, *97*, 23–34.
- (47) Leitl, M. J.; Zink, D. M.; Schinabeck, A.; Baumann, T.; Volz, D.; Yersin, H. Copper(I) Complexes for Thermally Activated Delayed Fluorescence: From Photophysical to Device Properties. *Top. Curr. Chem.* **2016**, 374, 25.
- (48) Lumpkin, R. S.; Kober, E. M.; Worl, L. A.; Murtaza, Z.; Meyer, T. J. Metal-to-Ligand Charge-Transfer (MLCT) Photochemistry. Experimental Evidence for the Participation of a Higher Lying MLCT State in Polypyridyl Complexes of Ruthenium(II) and Osmium(II). *J. Phys. Chem.* **1990**, *94*, 239–243.
- (49) Huang, L.-M.; Tu, G. M.; Chi, Y.; Hung, W. Y.; Song, Y. C.; Tseng, M. R.; Chou, P. T.; Lee, G. H.; Wong, K. T.; Cheng, S. H.; Tsai, W. S. Mechanoluminescent and efficient white OLEDs for Pt(II) phosphors bearing spatially encumbered pyridinyl pyrazolate chelates. *J. Mater. Chem. C* 2013, *1*, 7582–7592.
- (50) Fu, J.-Z.; Zhang, X.; Wang, J.-Y.; Zhang, L.-Y.; Chen, Z.-N. Synthesis and photophysical properties of cyclometallated iridium (III) acetylide complexes. *Inorg. Chem. Commun.* **2012**, 22, 123–125.
- (51) Chow, P.-K.; To, W.-P.; Low, K.-H.; Che, C.-M. Luminescent Palladium(II) Compleses with π Extended Cyclometalated [R- $\hat{C}\hat{N}N-R'$] and Pentafluorophenylacetylide Ligands: Spectroscopic, Photophysical, and Photochemical Properties. *Chem.—Asian J.* **2013**, *9*, 534–545.
- (52) Tong, G. S. M.; Law, Y.-C.; Kui, S. C. F.; Zhu, N.; Leung, K. H.; Phillips, D. L.; Che, C.-M. Ligand-to-Ligand Charge-Transfer Transitions of Platinum(II) Complexes with Arylacetylide Ligands

- with Different Chain Lengths: Spectroscopic Characterization, Effect of Molecular Conformations, and Density Functional Theory Calculations. *Chem.—Eur. J.* **2010**, *16*, 6540–6554.
- (53) Rossi, E.; Colombo, A.; Dragonetti, C.; Righetto, S.; Roberto, D.; Ugo, R.; Valore, A.; Williams, J. A. G.; Lobello, M. G.; De Angelis, F.; Fantacci, S.; Ledoux-Rak, I.; Singh, A.; Zyss, J. Tuning the Dipolar Second-Order Nonlinear Optical Properties of Cyclometalated Platinum(II) Complexes with Tridentate NĈN Binding Ligands. Chem.—Eur. J. 2013, 19, 9875–9883.
- (54) Eddy, L. E.; Thakker, P. U.; McMillen, C. D.; Pienkos, J. A.; Cordoba, J. J.; Edmunds, C. E.; Wagenknecht, P. S. A comparison of the metal-ligand interactions of the pentafluorophenylethynyl and trifluoropropynyl ligands in transition metal cyclam complexes. *Inorg. Chim. Acta* **2019**, *486*, 141–149.
- (55) Constable, E. C.; Henney, R. P. G.; Leese, T. A.; Tocher, D. A. Cyclometalation reactions of 5-phenyl-2,2'-bipyridine; a potential C,N,N-donor analog of 2,2':6',2''-terpyridine. Crystal and molecular structure of dichlorobis(6-phenyl-2,2'-bipyridine)ruthenium(II). *J. Chem. Soc., Dalton Trans.* 1990, 2, 443–449.
- (56) Frisch, M. J.; Trucks, G. W.; Schlegel, H. B.; Scuseria, G. E.; Robb, M. A.; Cheeseman, J. R.; Scalmani, G.; Barone, V.; Petersson, G. A.; Nakatsuji, H.; Li, X.; Caricato, M.; Marenich, A. V.; Bloino, J.; Janesko, B. G.; Gomperts, R.; Mennucci, B.; Hratchian, H. P.; Ortiz, J. V.; Izmaylov, A. F.; Sonnenberg, J. L.; Williams-Young, D.; Ding, F.; Lipparini, F.; Egidi, F.; Goings, J.; Peng, B.; Petrone, A.; Henderson, T.; Ranasinghe, D.; Zakrzewski, V. G.; Gao, J.; Rega, N.; Zheng, G.; Liang, W.; Hada, M.; Ehara, M.; Toyota, K.; Fukuda, R.; Hasegawa, J.; Ishida, M.; Nakajima, T.; Honda, Y.; Kitao, O.; Nakai, H.; Vreven, T.; Throssell, K.; Montgomery, J. A., Jr.; Peralta, J. E.; Ogliaro, F.; Bearpark, M. J.; Heyd, J. J.; Brothers, E. N.; Kudin, K. N.; Staroverov, V. N.; Keith, T. A.; Kobayashi, R.; Normand, J.; Raghavachari, K.; Rendell, A. P.; Burant, J. C.; Iyengar, S. S.; Tomasi, J.; Cossi, M.; Millam, J. M.; Klene, M.; Adamo, C.; Cammi, R.; Ochterski, J. W.; Martin, R. L.; Morokuma, K.; Farkas, O.; Foresman, J. B.; Fox, D. J. Gaussian 16, Revision C.01; Gaussian Inc.: Wallingford, CT, 2016.
- (57) Becke, A. D. Density-functional exchange-energy approximation with correct asymptotic behavior. *Phys. Rev. A: At., Mol., Opt. Phys.* **1988**, 38, 3098–3100.
- (58) Rassolov, V. A.; Ratner, M. A.; Pople, J. A.; Redfern, P. C.; Curtiss, L. A. 6-31G* Basis Set for Third-Row Atoms. *J. Comput. Chem.* **2001**, 22, 976–984.
- (59) Dunning, T. H.; Hay, P. J. In *Modern Theoretical Chemistry*; Schaefer, H. F., Ed.; Plenum: New York, 1977; Vol. 3, pp 1–28.
- (60) Dennington, R.; Keith, T. A.; Millam, J. M. Gauss View, Version 6; Semichem Inc.: Shawnee Mission, KS, 2016.
- (61) O'Boyle, N. M.; Tenderholt, A. L.; Langner, K. M. cclib: A library for package-independent computational chemistry algorithms. *J. Comput. Chem.* **2008**, *29*, 839–845.
- (62) APEX 3, Version 2017.3; Bruker-AXS Inc.: Madison, WI, 2017.
- (63) Sheldrick, G. M. Crystal structure refinement with SHELXL. *Acta Crystallogr., Sect. C: Struct. Chem.* **2015**, *71*, 3–8.
- (64) Sonogashira, K.; Fujikura, Y.; Yatake, T.; Toyoshima, N.; Takahashi, S.; Hagihara, N. Synthesis and properties of cis- and transdialkynyl complexes of platinum(II). *J. Organomet. Chem.* **1978**, *145*, 101–108.
- (65) Hissler, M.; Connick, W. B.; Geiger, D. K.; McGarrah, J. E.; Lipa, D.; Lachicotte, R. J.; Eisenberg, R. Platinum Diimine Bis(acetylide) Complexes: Synthesis, Characterization, and Luminescence Properties. *Inorg. Chem.* **2000**, *39*, 447–457.
- (66) Lin, J.; Zou, C.; Zhang, X.; Gao, Q.; Suo, S.; Zhuo, Q.; Chang, X.; Xie, M.; Lu, W. Highly phosphorescent organopalladium(II) complexes with metal-metal-to-ligand charge-transfer excited states in fluid solutions. *Dalton Trans.* **2019**, *48*, 10417–10421.
- (67) Poater, A.; Moradell, S.; Pinilla, E.; Poater, J.; Solà, M.; Martínez, M. Á.; Llobet, A. A trinuclear Pt(II) compound with short Pt-Pt-Pt contacts. An analysis of the influence of π - π stacking interactions on the strength and length of the Pt-Pt bond. *Dalton Trans.* **2006**, 1188–1196.

Inorganic Chemistry Article pubs.acs.org/IC

- (68) Chakraborty, S.; Aliprandi, A.; De Cola, L. Multinuclear Pt^{II} Complexes: Why Three is Better than Two to Enhance Photophysical Properties. Chem.—Eur. J. 2020, 26, 11007-11012.
- (69) Sengul, A. Crystal Structure of Nitrato (2,2',2"-terpyridyl)platinum(II) Hrdrogen Dinitrate, [Pt(terpy)ONO₂][H(ONO₂)₂]. Turk. J. Chem. 2005, 29, 571-578.
- (70) Phillips, V.; Willard, K. J.; Golen, J. A.; Moore, C. J.; Rheingold, A. L.; Doerrer, L. H. Electronic Influences on Metallophilic Interactions in $[Pt(tpy)X][Au(C_6F_5)_2]$ Double Salts. Inorg. Chem. **2010**, *49*, 9265–9274.
- (71) Sivchik, V.; Kochetov, A.; Eskelinen, T.; Kisel, K. S.; Solomatina, A. I.; Grachova, E. V.; Tunik, S. P.; Hirva, P.; Koshevoy, I. O. Modulation of metallophilic and π - π interactions in platinum cyclometalated luminophores with halogen bonding. Chem.—Eur. J. 2021, 27, 1787-1794.
- (72) Wan, K.-T.; Che, C.-M.; Cho, K.-C. Inorganic Excimer. Spectroscopy, Photoredox Properties and Excimeric Emission of Dicyano(4,4'-di-tert-butyl-2,2'- bi pyridine)platinum(1). Dalton Trans. 1991, 1077-1080.
- (73) Lai, S.-W.; Chan, M. C.-W.; Cheung, T.-C.; Peng, S.-M.; Che, C. M. Probing d8-d8 Interactions in Luminescent Mono- and Binuclear Cyclometalated Platinum(II) Complexes of 6-Phenyl-2,2'bipyridines. Inorg. Chem. 1999, 38, 4046-4055.
- (74) Connick, W. B.; Geiger, D.; Eisenberg, R. Excited-State Self-Quenching Reactions of Square Planar Platinum(II) Diimine Complexes in Room-Temperature Fluid Solution. Inorg. Chem. 1999, 38, 3264-3265.
- (75) Crosby, G. A. Spectroscopic Investigations of Excited States of Transition-metal Complexes. Acc. Chem. Res. 1975, 8, 231-238.
- (76) Lee, W. W. S.; Wong, K. Y.; Li, X. M. Luminescent Dicyanoplatinum(II) Complexes as Sensors for the Optical Measurement of Oxygen Concentrations. Anal. Chem. 1993, 65, 255-258.
- (77) Kim, D.; Bredas, J. L. Triplet excimer formation in platinumbased phosphors: A theoretical study of the roles of Pt-Pt bimetallic interations and interligands π - π interactions. J. Am. Chem. Soc. 2009, 131, 11371-11380.
- (78) Develay, S.; Williams, J. A. G. Intramolecular excimers based on rigidly-linked platinum(II) complexes: intense deep-red triplet luminescence in solution. Dalton Trans. 2008, 4562-4564.
- (79) Liu, L.; Wang, X.; Wang, N.; Peng, T.; Wang, S. Bright, Multiresponsive, Sky-Blue Platinum(II) Phosphors Based on a Tetradentate Chelating Framework. Angew. Chem., Int. Ed. 2017, 56, 9160-9164.
- (80) Sun, C.; Thakker, P. U.; Khulordava, L.; Tobben, D. J.; Greenstein, S. M.; Grisenti, D. L.; Kantor, A. G.; Wagenknecht, P. S. Trifluoropropynyl as a Surrogate for the Cyano Ligand and Intense, Room-Temperature, Metal-Centered Emission from Its Rh(III)-Complex. Inorg. Chem. 2012, 51, 10477-10479.
- (81) Niehaus, T. A.; Hofbeck, T.; Yersin, H. Charge-transfer excited states in phosphorescent organo-transition metal compounds: a difficult case for time dependent density functional theory? RSC Adv. 2015, 5, 63318-63329.
- (82) London, H. C.; Whittemore, T. J.; Gale, A. G.; McMillen, C. D.; Pritchett, D. Y.; Myers, A. R.; Thomas, H. D.; Shields, G. C.; Wagenknecht, P. S. Ligand-to-Metal Charge-Transfer Photophysics and Photochemistry of Emissive d0 Titanocenes: A Spectroscopic and Computational Investigation. Inorg. Chem. 2021, 60, 14399-14409.
- (83) Morello, G. R. Accurate Prediction of Emission Energies with TD-DFT Methods for Platinum and Iridium OLED Materials. J. Mol. Model. 2017, 23, 174.
- (84) Tomasi, J.; Mennucci, B.; Cammi, R. Quantum Mechanical Continuum Solvation Models. Chem. Rev. 2005, 105, 2999-3094.
- (85) Czerwieniec, R.; Kowalski, K.; Yersin, H. Highly efficient thermally activated fluorescence of a new rigid Cu(I) complex [Cu(dmp)(phanephos)]. Dalton Trans. 2013, 42, 9826-9830.
- (86) Wacholtz, W. F.; Auerbach, R. A.; Schmehl, R. H. Independent Control of Charge-Transfer and Metal-Centered Excited States in Mixed-Ligand Polypyridine Ruthenium(II) Complexes via Specific Ligand Design. Inorg. Chem. 1986, 25, 227-234.

- (87) Lam, W. H.; Lam, E. S.-H.; Yam, V. W.-W. Computational Studies on the Excited States of Luminescent Platinum(II) Alkynyl Systems of Tridentate Pincer Ligands in Radiative and Nonradiative Processes. J. Am. Chem. Soc. 2013, 135, 15135-15143.
- (88) Zhou, X.; Pan, Q.-J.; Xia, B.-H.; Li, M.-X.; Zhang, H.-X.; Tung, A.-C. DFT and TD-DFT Calculations on the Electronic Structures and Spectroscopic Properties of Cyclometalated Platinum(II) Complexes. J. Phys. Chem. A 2007, 111, 5465-5472.
- (89) Fleetham, T.; Ecton, J.; Wang, Z.; Bakken, N.; Li, J. Single-Doped White Organic Light-Emitting Device with an External Ouantum Efficiency Over 20%. Adv. Mater. 2013, 25, 2573-2576.
- (90) Bachmann, M.; Suter, D.; Blacque, O.; Venkatesan, K. Tunable and Efficient White Light Phosphorescent Emission Based on Single Component N-Heterocyclic Carbene Platinum(II)Complexes. Inorg. Chem. 2016, 55, 4733-4745.
- (91) Li, J. White OLEDs employing blue fluorescent emitters and orange phosphorescent excimers. U.S. Patent 20,220,013,733 A1,
- (92) Okamura, N.; Maeda, T.; Fujiwara, H.; Soman, A.; Unni, K. N. N.; Ajayaghosh, A.; Yagi, S. Photokinetic study on remarkable excimer phosphorescence from heteroleptic cyclometalated platinum(II) complexes bearing a benzoylated 2-phenylpyridinate ligand. Phys. Chem. Chem. Phys. 2018, 20, 542-552.

□ Recommended by ACS

Strategy for Achieving Long-Wavelength Near-Infrared Luminescence of Diimineplatinum(II) Complexes

Meng-Meng Su, Jun Ni, et al.

FERRIJARY 22 2021

INORGANIC CHEMISTRY

READ **C**

Solution-Processed Organic Light-Emitting Diodes of Yellow-Emitting PtAg, Complexes with an External **Quantum Efficiency of 21.7%**

Zhao-Yi Wang, Zhong-Ning Chen, et al.

AUGUST 03, 2021

ENERGY & FUELS

READ **C**

Synthetic Strategy for Preserving Sky-Blue Electrophosphorescence in Square-Planar Pt(II) **Complexes**

Yu Kyung Moon, Youngmin You, et al.

FERRUARY 04 2020

ACS APPLIED ELECTRONIC MATERIALS

READ **C**

Tuning State Energies for Narrow Blue Emission in Tetradentate Pyridyl-Carbazole Platinum Complexes

Tyler Fleetham, Mark E. Thompson, et al.

SEPTEMBER 05, 2019

INORGANIC CHEMISTRY

READ **C**

Get More Suggestions >